PCCP

Determination of the intermolecular geometry of the phenol–methanol cluster

A. Westphal,[a] Ch. Jacoby,[b] Ch. Ratzer,[a] A. Reichelt[a] and M. Schmitt*[a]

[a] *Heinrich-Heine-Universität, Institut für Physikalische Chemie, 40225, Düsseldorf, Germany. E-mail: mschmitt@uni-duesseldorf.de*
[b] *Institut für Herz- und Kreislaufphysiologie, Heinrich-Heine-Universität, Düsseldorf, Germany*

Received 25th June 2003, Accepted 15th August 2003
First published as an Advance Article on the web 5th September 2003

From the rovibronic spectrum of three isotopomers of the hydrogen bonded binary phenol–methanol cluster the inertial parameters have been determined. The geometry of the hydrogen bond was obtained from a fit of the six intermolecular geometry parameters to the rotational constants of these isotopomers and was compared to the results of *ab initio* calculations. The hydrogen bond length was found to decrease by 5 pm upon electronic excitation, due to the increased acidity of phenol in the S_1-state. The same fact is responsible for the increased linearity of the hydrogen bond in the S_1-state. The spectra of all three isotopomers are split by the interaction of the internal torsion of the methyl group with the overall rotation. Using the subtorsional splittings and the torsion–rotation parameters, the reduced barrier to internal rotation of the methyl group in the methanol moiety of the cluster could be determined to be 32.2 in the S_0-state and 27.9 in the S_1-state. This reduction can be traced back to the increased acidity of phenol in the S_1-state, which reduces the hyperconjugation between the methanolic oxygen σ-type lone pair and the hydrogen atoms of the methyl group.

1. Introduction

Hydrogen bonded clusters of phenol with methanol have been investigated in great detail both experimentally and theoretically, because they serve as ideal model systems for the examination of competing van der Waals and hydrogen bond interactions in a single supermolecular system.[1–6] The phenol–methanol structure is the result of a sensitive balance between dipole interactions, mainly responsible for the hydrogen bond and dispersive interactions, which describe the attractive forces between the methyl group and the π-system. These competing interactions play a crucial role, *e.g.* in the stabilization of the DNA structure, in which hydrogen bonding between base pairs and π-stacking of bases both contribute to the final helical structure.

The vibrational frequencies of the phenol–methanol cluster in the electronic ground state were determined by dispersed fluorescence spectroscopy by Abe *et al.*[2] The fluorescence excitation spectrum was measured and the vibronic bands assigned by Abe *et al.*[1] Recently, a joint spectroscopic and *ab initio* study on the intermolecular vibrations of several isotopomers of phenol–methanol was published by our group.[7] A theoretical analysis of the intermolecular vibrations in the electronic ground state was given by Gerhards *et al.*[4] They predicted a translinear geometry, as in the case of the phenol–water cluster. Courty *et al.* presented a structure of the cluster in which the methanolic methyl group is bent towards the aromatic ring resulting in a nonlinear hydrogen bond. This structure is based on a semi-empirical model potential.[6] In order to confirm, that only one conformer of phenol $(CH_3OH)_1$ is responsible for absorptions in the observed spectral region, hole burning spectroscopy (SHB) was performed.[5] Recently, a Fourier transform microwave spectrum of the phenol–methanol cluster was measured in the group of Stahl,[8] yielding rotational and centrifugal constants for the electronic ground state. In two preceding publications we determined details of the structure of the phenol–methanol cluster by rotationally resolved UV spectroscopy[9] of phenol $(CH_3OH)_1$ and by a comparison of the so determined structure with the results of *ab initio* calculations.[10]

From the analysis of the rotationally resolved spectrum we could determine the position of the methanol moiety in the inertial frame of the cluster. In conjunction, the rotation–internal rotation coupling and the inertial parameters yielded additional information on the intermolecular geometry of the hydrogen bond.

In the present publication we focus on the exact determination of the intermolecular geometry using the rotational constants of two other isotopomers of the cluster. This determination relies on the knowledge of the monomer structures of phenol and methanol. Both were examined thoroughly by microwave spectroscopy in the electronic ground state. Recently, we published the structure of phenol in the electronically excited state,[11] which now allows for an improved accuracy of the determination of the cluster structures in the S_1-state.

2. Results and discussion

The internal rotation of the methyl group of the hydrogen bonded phenol–methanol cluster gives rise to a torsional splitting in the electronic spectrum of the cluster. This splitting was observed in the high resolution spectrum of the electronic origin of phenol $(CH_3OH)_1$, as well as in the hole burning spectra, which were obtained *via* excitation of a single torsional component in the vibronic spectrum.[7]

All isotopomers of phenol–methanol dealt with in this publication, belong to the molecular symmetry group G_3. The lowest torsional wave function of a threefold internal rotor in the MS group G_3 transforms as A, the next transforms as E. The torsional wave functions can be expanded in the basis of free rotor functions:

$$|v,\sigma\rangle = \sum_{k=-\infty}^{\infty} A_{3k+\sigma}^{(v)} e^{i(3k+\sigma)\alpha} \qquad (1)$$

 DOI: 10.1039/b307223a

where v is the torsional state index and the integer σ takes on the values 0 and ± 1 for A and E levels, respectively. k runs over a limited number of basis functions. Generally 50 to 100 basis functions are sufficient for an accuracy of 0.1 cm^{-1} in the determination of the energy of the torsional levels. The selection rule for torsional transitions is $\Delta\sigma = 0$, because the transition dipole moment is independent of the torsional angle α for the symmetric rotors $-CH_3$ and $-CD_3$, which results in the observed transitions $A \leftrightarrow A$ and $E \leftrightarrow E$. The experimentally determined A–E splitting in the spectrum of the electronic origin is the difference between the $A \leftrightarrow A$ and $E \leftrightarrow E$ rovibronic origin frequencies.

The nuclear spin wave functions Ψ_{ns} transform as $4A + 2E$ for the $-CH_3$ group and as $11A + 8E$ for $-CD_3$. The overall wave functions for both rotors transform as A, thus the spin statistical weights of the A and E subbands are 1:1 for phenol $(CH_3OH)_1$ and 11:16 for phenol $(CD_3OH)_1$ and [7-D]phenol $(CD_3OD)_1$.

Traces a, c and e of Fig. 1 show the R2PI spectra of phenol $(CH_3OH)_1$, phenol $(CD_3OH)_1$, and [7-D]phenol $(CD_3OD)_1$ in the region of the intermolecular vibrations, the traces b, d, and f show the respective high resolution LIF spectra of the electronic origins.

At first sight, the rotationally resolved spectra of the electronic origins of phenol $(CD_3OH)_1$ and [7-D]phenol $(CD_3OD)_1$ seem to be less congested, compared to phenol $(CH_3OH)_1$. The reason is a very small splitting of the subtorsional components, leaving a spectrum, which resembles closely the spectrum of an unperturbed rigid rotor. We performed an autocorrelation of the experimental spectra, in order to obtain the subtorsional splittings. Fig. 2 shows the results of the autocorrelations of the electronic origins of phenol $(CH_3OH)_1$, phenol $(CD_3OH)_1$, and [7-D]phenol $(CD_3OD)_1$. In addition to the autocorrelation peak at zero lag, a broad, not very marked side peak is found for phenol $(CH_3OH)_1$ at a distance of 3550 MHz, in excellent agreement with the splitting determined from an assigned fit of the rovibronic spectrum.[9] For phenol $(CD_3OH)_1$ the side peak is almost as narrow as the autocorrelation peak and has a considerably high intensity. The subtorsional splitting in this case amounts to 440 MHz. Such a narrow, intense side peak in the autocorrelation function is an indication of very similar subspectra, *i.e.* very similar molecular constants of the subspectra. In the case of [7-D]phenol $(CD_3OD)_1$ no side peak can be found at first sight. Closer inspection of the autocorrelation peak shows, that it is comprised of the main band at zero frequency lag and two side lobes at approximately 70 MHz. Also in this case the side peaks are narrow and intense, indicating similar torsional subspectra.

Using the information about the size of the subtorsional splitting, it is quite straightforward to assign the rovibronic lines of each of the isotopic clusters, although the individual spectra are rather congested. The frequencies of the A-rovibronic lines were fit to the Hamiltonian for a distortable rotor in Watson's A-reduced form:[12,13]

$$\begin{aligned}\hat{H}_{v\sigma}^{(A)} = {} & A_{v\sigma}P_a^2 + B_{v\sigma}P_b^2 + C_{v\sigma}P_c^2 \\ & - \Delta_J P^4 - \Delta_{JK} P^2 P_a^2 - \Delta_K P_a^4 \\ & - 2\delta_J P^2 (P_b^2 - P_c^2) - \delta_K \left[P_a^2 (P_b^2 - P_c^2) \right. \\ & \left. + (P_b^2 - P_c^2) P_a^2 \right] \end{aligned} \quad (2)$$

in which the effective rotational constants $A_{v\sigma}$, *etc.* incorporate the second order torsional perturbation coefficients for a given torsional state $|v,\sigma\rangle$.[9] The E-rovibronic lines were fit to the Hamiltonian from eqn. (2), which is extended by the

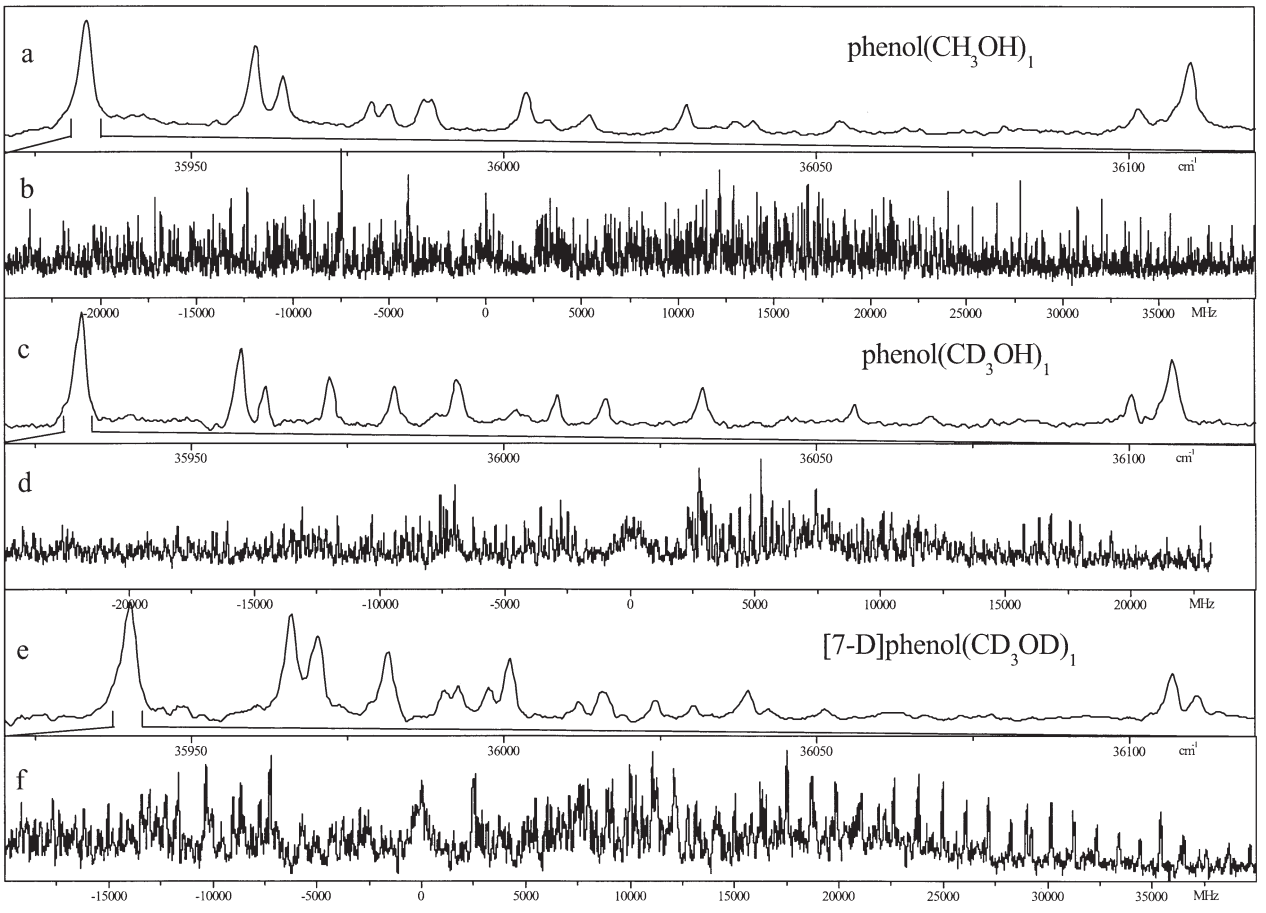

Fig. 1 R2PI spectra (trace a, c, e) of three isotopomers of the phenol–methanol cluster in the region of the intermolecular vibrations and corresponding HRLIF spectra (trace b, d, f) of the electronic origins.

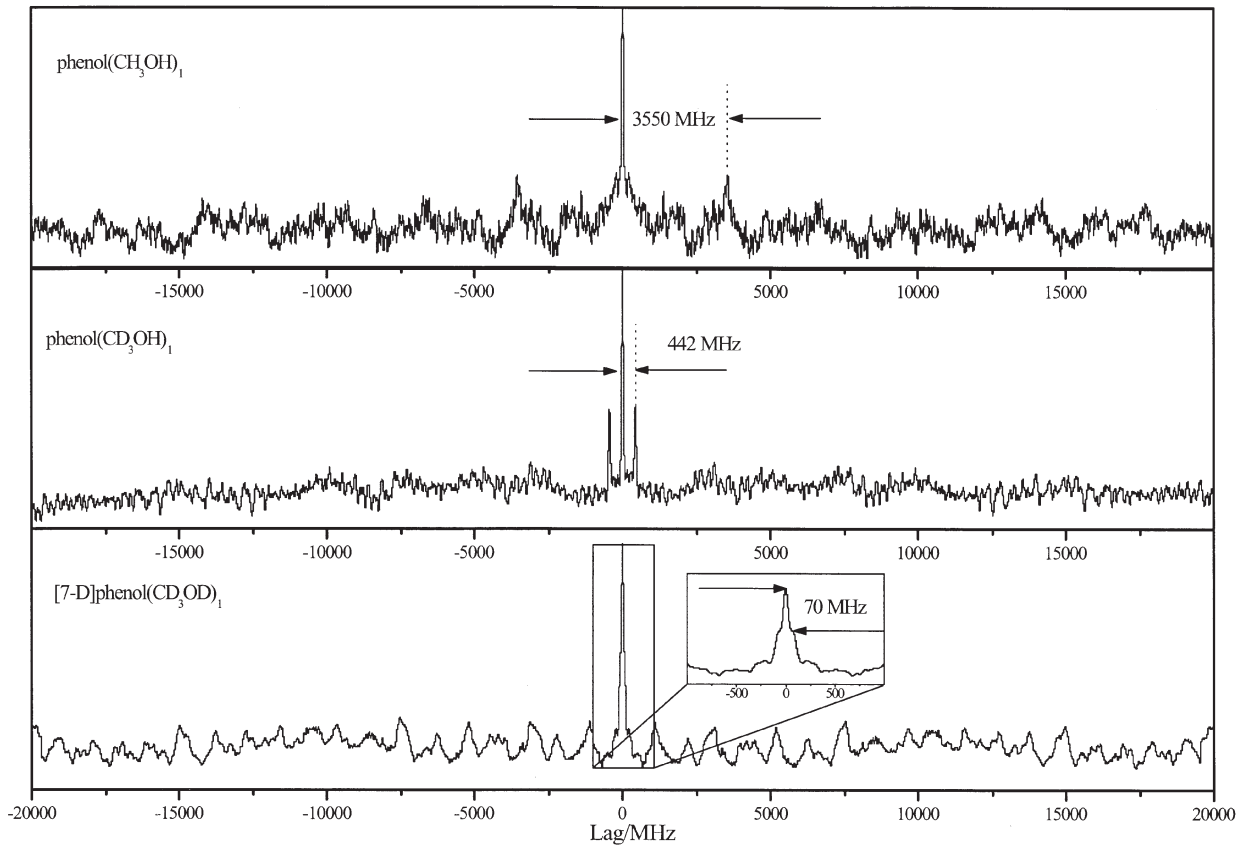

Fig. 2 Autocorrelation of the rotationally resolved LIF spectra of the electronic origins of phenol $(CH_3OH)_1$, phenol $(CD_3OH)_1$ and [7D]-phenol $(CD_3OD)_1$.

torsion–rotation parameters D_g, which are the coefficients of linear terms in the overall angular momenta P_g:[14,15]

$$\begin{aligned}\hat{H}_{v\sigma}^{(E)} &= A_{v\sigma}P_a^2 + B_{v\sigma}P_b^2 + C_{v\sigma}P_c^2 \\ &\quad - \Delta_J P^4 - \Delta_{JK}P^2P_a^2 - \Delta_K P_a^4 \\ &\quad - 2\delta_J P^2(P_b^2 - P_c^2) - \delta_K\left[P_a^2\left(P_b^2 - P_c^2\right)\right. \\ &\quad \left. + \left(P_b^2 - P_c^2\right)P_a^2\right] \\ &\quad + D_aP_a + D_bP_b + D_cP_c \end{aligned} \quad (3)$$

Figs. 3 and 4 show the rotationally resolved electronic origins of phenol $(CD_3OH)_1$ and [7-D]phenol $(CD_3OD)_1$ along with the fits of both subtorsional components. In Table 1 the inertial parameters of phenol $(CD_3OH)_1$, [7-D]phenol $(CD_3OD)_1$ and for comparison also the previously published parameters of phenol $(CH_3OH)_1$ are reported, which were obtained from the fit. For [7-D]phenol $(CD_3OD)_1$ the torsion–rotation parameters D_g were too small to be determined. For phenol $(CD_3OH)_1$ our fit did not converge when the torsion–rotation constant D_b was included in the fit. Nevertheless, fits with all D_g fitted, but D_b set to zero in both electronic states, resulted in the lowest χ^2.

The subtorsional splittings determined from the assigned line fits are in good agreement with the values, which are observed in the autocorrelation functions of the rovibronic spectra (Fig. 2). The relative intensities of the bands are difficult to adjust, due to many overlapping rovibronic transitions, which contribute to the individual bands in the spectrum. Three factors have been considered, in order to reproduce the experimental intensities: the rotational temperature, the angle of the transition dipole moment with the inertial axes, and the nuclear spin statistics. The spin statistical weights are fixed to an intensity ratio of 11:16 for the A and E subbands of phenol $(CD_3OH)_1$ and [7-D]phenol $(CD_3OD)_1$, as explained above. The squared direction cosines of the transition dipole moment vector with the inertial axes have been calculated for phenol $(CD_3OH)_1$ and [7-D]phenol $(CD_3OD)_1$ using the geometry of phenol $(CH_3OH)_1$ from ref. 9. The transition dipole in the phenol moiety of the cluster is assumed to have the same direction as in the uncomplexed phenol monomer. The temperature has been adjusted by manually changing this parameter and inspection of the gross intensities in the simulated and experimental spectrum. It could be determined to be 1.5 K.

2.1. Intermolecular geometry

The effective rotational constants $A_v\sigma$, *etc.*, which are given in Table 1 for the A- and the E-states (the torsional state under consideration here is $v = 0$ in S_0 and S_1-state.) have to be corrected for the torsional perturbation, in order to obtain the geometric rotational constants. They are obtained as the weighted means of the $\sigma = 0$ and $\sigma = 1$ inertial parameters:

$$A = \frac{1}{3}A_{v0} + \frac{2}{3}A_{v1} \quad etc. \quad (4)$$

The so determined geometric rotational constants for phenol $(CH_3OH)_1$ (h_5), phenol $(CD_3OH)_1$ (d_3) and [7-D]phenol $(CD_3OD)_1$ (d_5), which are used for the structure determination are given in Table 2. The determination of geometries from rotational constants depend critically upon the correlation which might exist between the inertial parameters. As the rovibronic spectra are of $a/b/c$-type there are no redundancies in the determination of the inertial parameters. The correlation matrix which gives indications for dependences between the parameters has been checked and no off-diagonal elements greater than 0.8 are found, so that the parameters can be viewed as independent.

The relative orientation of the phenol and the methanol moiety can be described by six geometry parameters (one

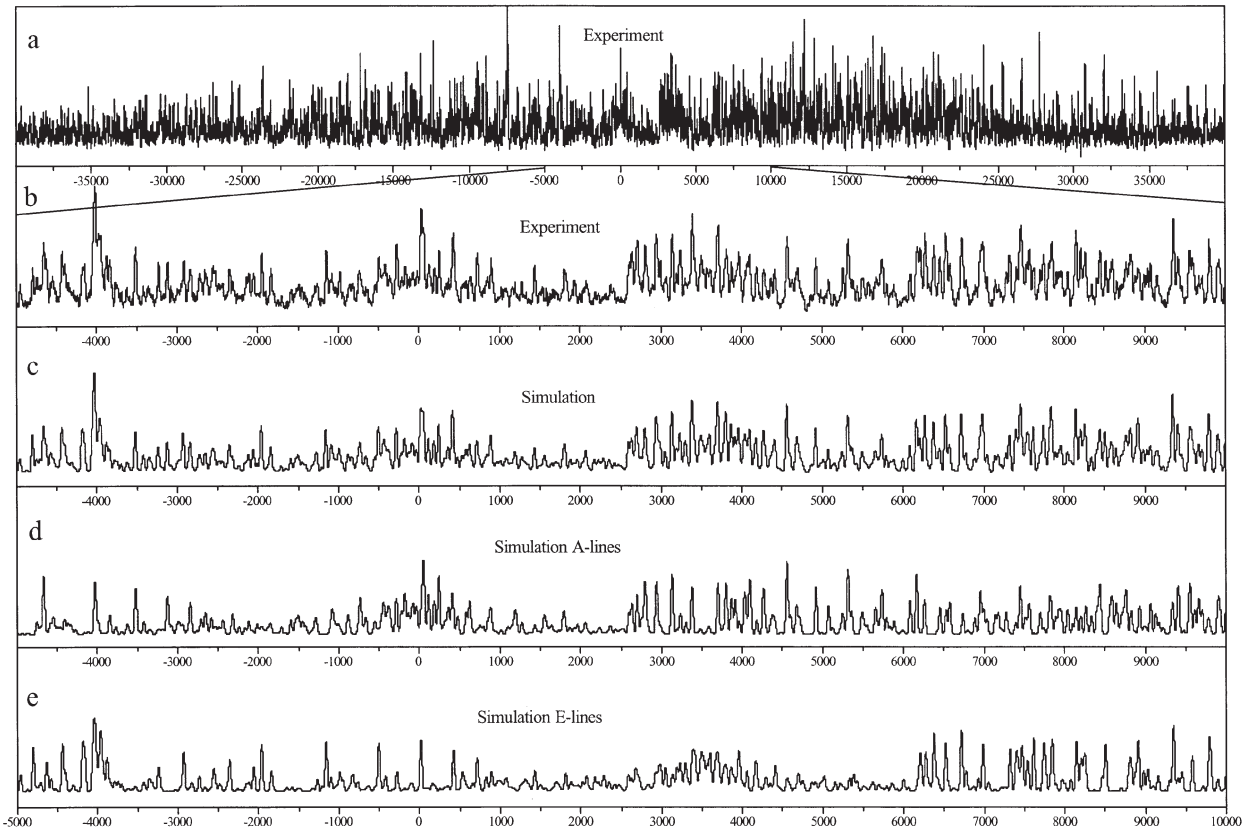

Fig. 3 Rotationally resolved LIF spectrum of phenol $(CD_3OH)_1$ along with the simulation, using the parameters from Table 1. The individual traces show (a) the experimental rovibronic spectrum of the electronic origin; (b) expanded part of (a) from −5000 to +10 000 MHz around the origin of the $\sigma = 0$ torsional component; (c) the simulation as the sum of the $\sigma = 0$ and $\sigma = 1$ torsional components with spin statistical weights of 11:16; (d) the simulation of the $\sigma = 0$ torsional component; (e) the simulation of the $\sigma = 1$ torsional component.

distance, two angles, and three dihedral angles). The structure of the phenol moiety in the electronic ground state of the cluster is constrained to the geometry, determined by microwave spectroscopy by Larsen,[16] and in the electronically excited state to the S_1-state geometry, determined by Ratzer *et al.* using HRLIF.[11] The structure of the methanol moiety is supposed not to change upon electronic excitation and has been kept fixed for both electronic states to the MW-geometry, determined by Gerry *et al.*[17]

We defined the internal coordinates of the cluster as shown in Fig. 5 and fitted the six intermolecular parameters to the nine rotational constants of three isotopomers, using our self developed program *pKrFit*.[11] Geometry models, which can be utilized with this program are the r_0-geometry, which neglects vibrational effects from the different isotopomers, the pseudo-r_s-structures,[18] which consider vibrational effects through equal vibrational contributions for all isotopomers; and Watsons mass weighted $r_m^{(1)}$ and $r_{m;}^{(2)}$-structures.[19–22]

The r_0-intermolecular structures for both electronic states have been determined using the geometric rotational constants from (h_5), (d_3), (d_5)-phenol–methanol. Tables 3 and 4 display the results of the fit for both electronic states, along with the results of several *ab initio* calculations and a geometry optimization using a semi-empirical model potential[6] on this cluster. For a fit of the intermolecular pseudo-r_s or $r_m^{(1)}$-structure nine rotational constants are not sufficient, because already six rotational constants are needed for a fit of the geometry parameters and three more parameters have to be fit to include the vibrational contributions of each isotopomer.

The comparison of the experimentally determined structure and calculated structures at the MP2/6-311G(d,p) level of theory and using a semi-empirical model potential (taken from ref. 6) show good agreement (*cf.* Fig. 6 and Table 3). The semi-empirical structure which is shown is a rotamer with respect to the phenolic OH-group, which is energetically equivalent to the rotamers given in Fig. 6 (a) and (b). The structure obtained with the model potential, in particular, reproduces the one determined experimentally to a high degree of accuracy. The hydrogen bond length, which is underestimated at the MP2 level, is predicted quite well from the semi-empirical model.

Inspection of Tables 3 and 4 shows, that the hydrogen bond distance d between phenol and methanol decreases by 5 pm upon electronic excitation. This can be explained by the increased acidity of phenol in the S_1-state and the stronger interaction with the methanol moiety, which acts as a base in this cluster. The angle a_2, which is defined by O_P–H_P–O_M shows a larger deviation from linearity for the ground state of the cluster, compared to the electronically excited state. Also this fact can be attributed to the increased acidity and therefore the increased interaction. The position of the methanolic methyl group with respect to the aromatic ring can be inspected in Fig. 7. In the S_1-state the methanol moiety is bent slightly more towards the ring, indicating a stronger dispersive interaction in the electronically excited state of the cluster, what can be explained by the shift of electron density into the aromatic ring upon electronic excitation.

The *ab initio* calculations have been performed with the Gaussian98 program package (Revision11).[23] Due to the sensitive equilibrium of dispersive and dipole interactions which determine the intermolecular geometry, special care has to be taken in the geometry optimization. The different shape of counterpoise-corrected and counterpoise-uncorrected potential energy surfaces may lead to quite different equilibrium geometries[24] for hydrogen bonded complexes. The geometry optimizations have been performed with the equilibrium

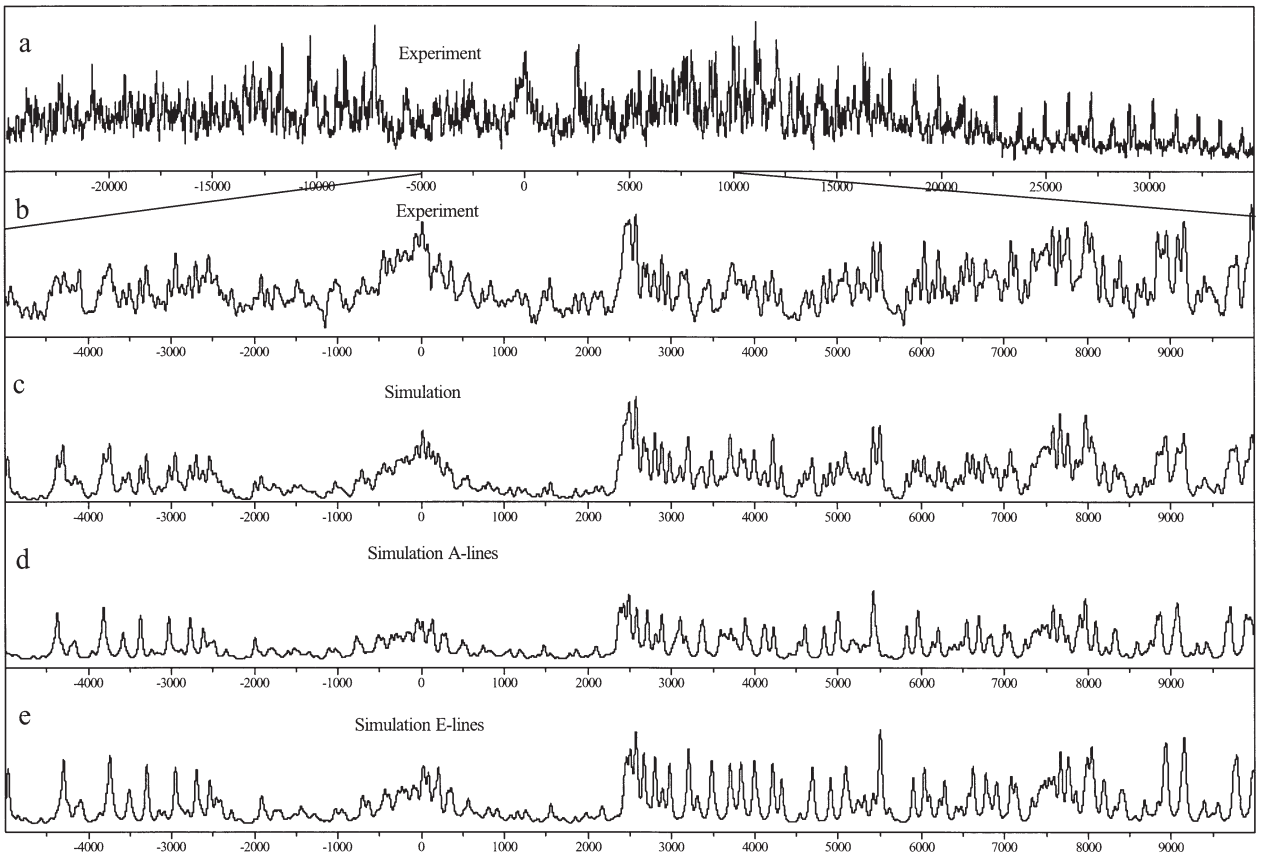

Fig. 4 Rotationally resolved LIF spectrum of [7-D]phenol $(CD_3OD)_1$ along with the simulation, using the parameters from Table 1. The individual traces show (a) the experimental spectrum; (b) expanded part of (a) from −5000 to +10 000 MHz around the origin of the $\sigma = 0$ torsional component; (c) the simulation as the sum of the $\sigma = 0$ and $\sigma = 1$ torsional components with spin statistical weights of 11:16; (d) the simulation of the $\sigma = 0$ torsional component; (e) the simulation of the $\sigma = 1$ torsional component.

geometries from ref. 10 as starting values and counterpoise corrected gradient optimizations, as implemented in Gaussian98.[23]

Table 5 shows the experimentally determined rotational constants along with the results of counterpoise corrected MP2 calculations, with the 6-31G(d,p) and the 6-311++G(d,p) basis sets and a CASSCF calculation with an active (12/9) space for the S_0-state. The active space comprises the six π-electrons in six benzene valence orbitals, two electrons in the phenolic oxygen lone pair orbital with π-symmetry and four electrons in two methanolic lone pair orbitals. Obviously CASSCF, which lacks electron–electron correlation is not capable of describing the structure of the cluster correctly, while the MP2 calculation does surprisingly well, considering the rather small basis set applied.

The MP2 rotational constants deviate considerably from the values, which were calculated at the same level of theory, but without a counterpoise corrected gradient optimization. Table 6 shows the comparison of the rotational constants with and without counterpoise corrected gradients. Generally the counterpoise corrected geometries, calculated at the correlated MP2 level have larger A rotational constants and smaller B and C rotational constants compared to the uncorrected geometries. The counterpoise correction for the uncorrelated HF optimization leads to virtually the same geometry as for the uncorrected optimization. The resulting HF structure can best be described as a translinear hydrogen bonded cluster, as in the case of phenol–water, because of a complete lack of correlation interaction in order to describe the dispersive forces in the cluster.

The rotational constants, determined at the MP2/6-311++G(d,p) level already reproduce the experimental rotational constants very well, with deviations of 6% in the A-constants and less than 2% in B and C.

2.2. Reduced barrier to internal rotation of the methyl group

The experimentally observed A–E splitting is a function of the difference of the reduced barrier height V_n/F in the two electronic states which are connected by the electronic transition. In a preceding publication[9] we determined the values of V_3/F to be 32.16 in the S_0-state and 27.65 in the S_1-state from a perturbation analysis of the electronic origin of phenol $(CH_3OH)_1$. These reduced barriers resulted in V_3-barriers for the methyl group torsion of 5084.6 GHz (170 cm^{-1}) for the electronic ground state and of 4374.5 GHz (146 cm^{-1}) for the electronically excited S_1-state under the assumption of a purely geometrically defined torsional constant F of 158 GHz.

The large change of the torsional barrier of methanol upon complexation was explained by a strong coupling of the torsional mode with the librational mode of the cluster. The analysis of the subtorsional splitting of phenol $(CD_3OH)_1$ and [7-D]phenol $(CD_3OD)_1$ further supports this interpretation. If the torsional constant F would purely be defined by a rigid, symmetric top ($-CH_3$, $-CD_3$) and a rigid, asymmetric frame (the rest of the cluster), the reduced barrier height of phenol $(CD_3OH)_1$ and [7-D]phenol $(CD_3OD)_1$ should be nearly the same in the S_0-state, as well as in the S_1-state. Consequently, the experimentally observed A–E splitting should be nearly the same for both isotopomers. The torsional constant F for a one-dimensional torsion is defined by:

$$F = \frac{h}{8\pi^2 r I_\alpha} \tag{5}$$

with

$$r = 1 - \sum_{g=a,b,c} \frac{\lambda_g^2 I_\alpha}{I_g} \tag{6}$$

Table 1 Effective rotational constants, centrifugal distortion and torsion–rotation constants of phenol $(CH_3OH)_1$,[9] phenol $(CD_3OH)_1$ and [7-D]phenol $(CD_3OD)_1$ in the ground and electronically excited states; the number of digits retained for each parameter were calculated according to the scheme of Watson,[33] so that the calculated standard deviation of the fit can be reproduced within 10%

	Phenol $(CH_3OH)_1$			
	S_0		S_1	
	A	E	A	E
$A_v\sigma$/MHz	3290.955(117)	3290.723(212)	3311.333(105)	3310.151(155)
$B_v\sigma$/MHz	792.126(80)	792.2965(901)	775.896(73)	775.8760(868)
$C_v\sigma$/MHz	685.8108(657)	685.4634(633)	664.3170(661)	664.2267(619)
Δ_J/kHz	0.313(246)	0.963(240)	0.207(228)	0.113(268)
Δ_{JK}/kHz	−5.17(113)	−5.51(245)	−3.82(108)	−0.17(18)
Δ_K/kHz	23.92(210)	18.26(503)	12.91(181)	5.57(306)
δ_J/kHz	0.002(145)	0.1106(1343)	0.096(132)	−0.0652(1397)
δ_{JK}/kHz	−17.2(144)	41.2(150)	−5.0(138)	−5.0(114)
D_a/MHz	—	32.83(34)	—	78.90(32)
D_b/MHz	—	14.3(78)	—	38.2(34)
D_c/MHz	—	40.312(183)	—	52.134(187)
ν_0/cm^{-1}			35932.85(2)	35932.97(2)
$\nu_0(E) - \nu_0(A) = 3557.621(740)$ MHz				
	Phenol $(CD_3OH)_1$			
$A_v\sigma$/MHz	3141.880(258)	3142.791(319)	3170.049(201)	3170.413(271)
$B_v\sigma$/MHz	747.671(184)	746.565(190)	729.649(243)	730.911(181)
$C_v\sigma$/MHz	653.864(182)	654.392(161)	631.636(203)	630.289(201)
Δ_J/kHz	1.09(10)	1.89(10)	0.03(14)	4.9(11)
Δ_{JK}/kHz	−21.3(54)	30.9(71)	−8.8(65)	3.4(75)
Δ_K/kHz	35.9(87)	−22.96(87)	26.1(69)	2.3(73)
δ_J/kHz	−0.05(836)	−1.07(437)	−1.84(94)	6.4(5)
δ_{JK}/kHz	5.6(560)	−302.7(508)	−104.8(847)	245.4(508)
D_a/MHz	—	0	—	0
D_b/MHz	—	6.95(304)	—	36.83(100)
D_c/MHz	—	3.82(38)	—	12.49(32)
ν_0/cm^{-1}			35932.12(2)	35932.14(2)
$\nu_0(E) - \nu_0(A) = 438.52(106)$				
	[7-D]Phenol $(CD_3OD)_1$			
$A_v\sigma$/MHz	3106.49(46)	3107.41(39)	3126.29(35)	3126.76(26)
$B_v\sigma$/MHz	728.422(199)	728.714(108)	712.278(195)	713.360(116)
$C_v\sigma$/MHz	638.934(183)	639.664(120)	619.908(170)	619.691(96)
Δ_J/kHz	−3.19(140)	−0.65(70)	−3.76(135)	−0.42(64)
Δ_{JK}/kHz	−18.49(939)	−2.28(58)	2.1(69)	−0.74(364)
Δ_K/kHz	−20.5(35)	38.2(185)	−23.6(196)	15.4(91)
δ_J/kHz	1.146(668)	0.825(379)	−1.32(95)	0.37(27)
δ_{JK}/kHz	71.9(548)	−43.5(292)	−130.9(511)	−20.9(272)
ν_0/cm^{-1}			35926.27(2)	35926.27(2)
$\nu_0(E) - \nu_0(A) = 76.10(90)$ MHz				

where I_α is the moment of inertia of the internal rotor, the λ_g are the direction cosines between the inertial axes and the axis of internal rotation and the I_g are the principal moments of inertia of the whole molecule. The moment of inertia of the CD_3 group I_α is 6.424 u Å^2 and all λ_g can be calculated from the experimentally determined structures of [7-D]phenol $(CD_3OD)_1$ and of phenol $(CD_3OD)_1$. Using the parameters

Table 2 Geometric rotational constants in MHz of three isotopomers of phenol–methanol

	S_0			S_1		
	h_5	d_3	d_5	h_5	d_3	d_5
A	3290.8(1)	3142.5(3)	3106.7(6)	3310.5(1)	3170.3(2)	3126.4(4)
B	792.19(7)	746.93(18)	728.72(21)	775.89(6)	730.49(14)	713.18(24)
C	685.62(5)	654.21(15)	639.74(20)	664.25(5)	630.74(9)	619.79(21)

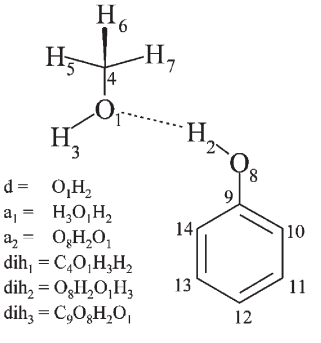

Fig. 5 Definition of the intermolecular internal coordinates of the phenol $(CH_3OH)_1$ cluster, used in the fit. The distances, angles, and dihedral angles given in this figure are not drawn to scale and do not belong to a meaningful geometry of the cluster. They are only given for sake of clarity of the definitions.

Table 3 Intermolecular S_0-state internal geometry parameters of the hydrogen bond of phenol–methanol as given in Fig. 5; d designates the distance $[O_1H_2]$, a_1 the angle $[O_8H_2O_1]$ and d_1 d_2 and d_3 the dihedral angles $[C_4O_1H_3H_2]$, $[O_8H_2O_1H_3]$, and $[C_9O_8H_2O_1]$, respectively; the monomer geometry of phenol in the electronic ground state has been taken from ref. 16; the methanol geometry has been set to the values of 17

	r_0	MP2 6-31G(d,p)	MP2 6-311++G(d,p)	CAS(12/9) 6-31G(d,p)	Semi-empirical[6]
d/pm	216.54(233)	195.99	192.38	195.86	209.13
a_1	104.7(149)	118.1	123.6	118.9	110.3
a_2	166.3(11)	167.3	167.0	173.9	165.2
d_1	−90.3(52)	−125.4	−135.0	−138.2	114.6
d_2	−126.3(26)	−110.0	−131.8	−128.9	100.6
d_3	−77.6(20)	−100.3	−76.3	−119.6	100.1

from Table 1 and barriers of 170 cm^{-1} and 146 cm^{-1} for the S_0 and S_1-state, respectively, the maximum difference of the A – E splitting for [7-D]phenol $(CD_3OD)_1$ and phenol $(CD_3OD)_1$ should amount to less than 1 MHz, if the motion was indeed a simple one-dimensional torsion. Nevertheless, we observed an A–E splitting of 76 MHz for [7-D]phenol $(CD_3OD)_1$ and of 438.52 MHz for phenol $(CD_3OD)_1$. This large difference, which cannot be explained by different torsional constants of the two isotopomers, points to a strong coupling of the torsion with a vibrational mode, which involves the methanolic and the phenolic hydroxy group. Therefore we decided to include only the torsional parameters of phenol $(CH_3OH)_1$ and phenol $(CD_3OD)_1$ in the fit of the barrier, which show the same isotopic substitution in the hydrogen bond.

The linear angular momentum terms D_a, D_b, and D_c, which are smaller for phenol $(CD_3OH)_1$ and for [7-D]phenol $(CD_3OD)_1$ than for phenol $(CH_3OH)_1$ can be used to improve the fit of the torsional barrier. They are defined by:

$$D_g = \frac{W^{(1)}_{v,\sigma}\lambda_g B_g}{r} \quad g = a, b, c \tag{7}$$

with $W^{(1)}_{v,\sigma} = W_{0,\pm1}{}^{(1)}$ as the first order perturbation coefficients for the E-levels of $v = 0$, and the B_g as the rotational constants of the cluster. The absolute values of the direction cosines λ_g are calculated from the experimentally determined structure (*cf.* section 2.1) under the assumption, that the torsional axis coincides with the C–O-bond of methanol. Their absolute values are given in Table 7. Their sign can in principle be inferred from an intensity analysis of the spectra, which was not possible in our case to their small absolute values.[9] The first order perturbation coefficients $W_{0,\pm1}{}^{(1)}$ are calculated using the torsional wavefunctions:[25]

$$W^{(1)}_{v,\sigma} = -2\mathrm{i}\int_0^{2\pi}\sum_{k=-\infty}^{\infty} A^{(v)}_{3k+\sigma}\mathrm{e}^{-\mathrm{i}(3k+\sigma)\alpha} \times \frac{\mathrm{d}}{\mathrm{d}\alpha}\sum_{k=-\infty}^{\infty} A^{(v)}_{3k+\sigma}\mathrm{e}^{\mathrm{i}(3k+\sigma)\alpha}\mathrm{d}\alpha \tag{8}$$

Table 4 Intermolecular S_1-state internal geometry parameters of the hydrogen bond of phenol–methanol as given in Fig. 5; d designates the distance $[O_1H_2]$, a_1 the angle $[H_3O_1H_2]$, a_1 the angle $[O_8H_2O_1]$ and d_1 $[O_8H_2O_1H_3]$, and $[C_9O_8H_2O_1]$, respectively; the monomer geometry of phenol in the electronic ground state has been taken from ref. 11; the methanol geometry has been set to the values given in the MW study of Gerry *et al.*[17]

	r_0	CIS 6-31G(d,p)	CAS(12/9) 6-31G(d,p)
d/pm	211.39(719)	189.05	194.58
a_1	76.0(190)	122.2	118.4
a_2	185.6(19)	168.5	173.4
d_1	−86.2(91)	−138.1	−137.1
d_2	−37.5(37)	−116.3	−115.1
d_3	−160.9(35)	−96.4	−129.3

where the eigenvector coefficients $A_{3k+\sigma}{}^{(v)}$ are obtained from the numerical solution of the pure torsional problem.

Thus, the torsion–rotation parameters D_g, depend on the (reduced) barrier height, and can be used as additional parameters in the fit of the reduced barrier to the experimentally determined subtorsional splittings. These subtorsional splittings are functions of the eigenvalues of the pure torsional Schrödinger equation, whereas the torsion–rotation parameters D_g, obtained from eqns. (7) and (8) are functions of the *eigenvector coefficients* $A_{3k+\sigma}{}^{(v)}$ of the torsional wavefunctions.

We set up a computer program for a simultaneous fit of the reduced barrier height in both electronic states to the experimentally determined A – E splittings and to the torsion–rotation parameters D_g of several isotopomers using the Levenberg–Marquardt algorithm.[26,27] Furthermore the program is capable of including the frequencies of torsional transitions, which are obtained from low resolution spectra of several isotopomers, in the fit of the barriers and torsional constants for both electronic states.[28]

The isotopomers used in our fit of the torsional barrier are phenol $(CH_3OH)_1$ and phenol $(CD_3OH)_1$, *vide supra*. The parameters used in the fit are compiled in Table 7. Using these parameters, the reduced barrier height to internal rotation of the methyl group could be determined to be 32.236 in the S_0-state and 27.906 in the S_1-state. For a purely geometric torsional constant of 158 GHz the torsional barriers are calculated to be 5093 and 4409 GHz, respectively.

The question arises, if the effect of barrier height decrease might be due to an increase in zero-point energy of the cluster

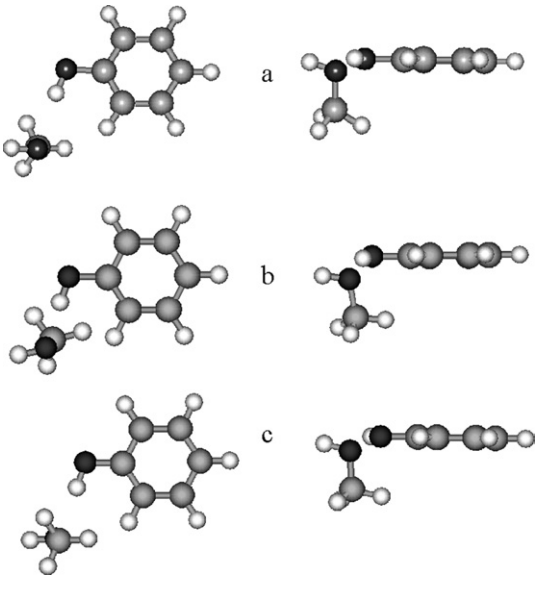

Fig. 6 (a) Experimental ground state structure of the phenol–methanol cluster. (b) MP2/6-311G(d,p) optimized structure. (c) Calculated semi-empirical structure from ref. 6.

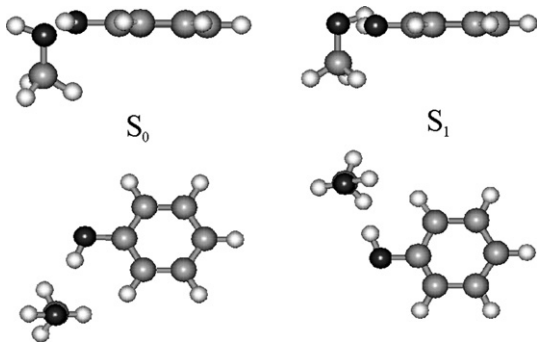

Fig. 7 Experimentally determined structure of phenol–methanol in the S_0- and in the S_1-state.

upon electronic excitation. This effect would be based on a coupling of the torsional motion to other vibrations, which is not included in our one-dimensional model. The total zero-point energy in the electronically excited state, calculated at the optimized CIS/6-311++G(d,p) level of theory is about 750 cm^{-1} smaller than in the electronic ground state (HF/6-311++G(d,p)). Of course there exist vibrations, that show an increase in ZPE along this special coordinate. If these coordinates couple more strongly to the torsion than vibrations which show a decrease in ZPE this might result in a reduction of barrier height upon electronic excitation. The most probable candidates for a coupling to the torsion are the low frequency intermolecular vibrational modes. The β_2 mode, which has considerable torsional character and is therefore most likely to couple to the torsion shows a calculated frequency shift upon electronic excitation of 18 cm^{-1}. We therefore conclude that ZPE effects on the barrier due to coupling to other modes should have a much smaller effect than observed in the experiment. It is therefore not a very likely candidate to explain the decrease in barrier height.

3. Conclusions

The intermolecular geometry of the phenol–methanol cluster could be determined by rotationally resolved LIF spectroscopy of three different isotopomers of the cluster. The structure is determined by a sensitive equilibrium between dipole–dipole and dispersive interactions. Using the nine rotational constants from three isotopomers, the six intermolecular geometry parameters could be determined. From these parameters we conclude that two competing interactions stabilize the phenol–methanol cluster and determine its structure. The dipole–dipole interaction tends to bind the methanol *via* a linear hydrogen bond to the proton donating hydroxy group of phenol (as in phenol–water), while dispersive interactions, mainly between the methyl group and the aromatic π-system (as in phenol–methane), result in a bent structure with the methyl group pointing in the direction of the aromatic ring. The dipole–dipole interaction is stronger in the electronically excited state due to the increased acidity of phenol in the S_1-state. The resulting larger dipole moment in the electronically excited state (0.59 D *vs.* 0.57 D) is found theoretically at the CASPT2 level,[29] although these calculations do not account for the complete change upon electronic excitation, because the S_0 and S_1-structures are not optimized at this level of theory. The results of the *ab initio* calculations are quite ambivalent, concerning the geometry in the ground and electronically excited state. While the ground state structure and rotational constants can be determined with an accuracy, that certainly helps in the assignment of the spectrum, the excited state structure is missed completely. This is not unexpected, as the inclusion of electron correlation for determination of the ground state structure of this cluster has been shown to be very important. Every method for calculation of the excited state which does not account for correlation effects, like CIS or CASSCF will fail inevitably.

The reduced torsional barrier of the methanol moiety drops from 32.2 to 27.9 upon electronic excitation in the phenol chromophore. If the origin of the change in the methyl torsional barrier were purely steric (Pauli exchange repulsion), one would expect an increase of barrier height upon electronic excitation in the phenol chromophore, because the distance between the phenolic π-system and the methyl group decreases. However, Pophristic *et al.*[30] pointed out, that the main reason for the torsional barrier in methanol is a vicinal hyperconjugation, involving the σ oxygen lone pair (of methanol) and the H-atoms of the methyl group in the staggered conformation.

Table 5 Experimental and calculated rotational constants of the phenol–methanol cluster

	S_0			
	Exp.	MP2 6-31G(d,p)	MP2 6-311++G(d,p)	CAS(12,9) 6-31G(d,p)
A/MHz	3290.8(1)	3390	3099	3749
B/MHz	792.19(7)	748	805	687
C/MHz	685.62(5)	648	696	602
	S_1			
A/MHz	3310.5(1)	—	—	3596
B/MHz	775.89(6)	—	—	685
C/MHz	664.25(5)	—	—	597
ΔA/MHz	+19.7	—	—	−153
ΔB/MHz	−16.3	—	—	−2
ΔC/MHz	−21.4	—	—	−5

Table 6 Comparison of counterpoise corrected and uncorrected gradient optimizations for the phenol–methanol cluster

		MP2		MP2		HF	
		6-31G(d,p)		6-311++G(d,p)		6-311++G(d,p)	
	Exp.	non-cp	cp	non-cp	cp	non-cp	cp
A/MHz	3290.8	3220	3390	2954	3099	3812	3832
B/MHz	792.19	845	748	885	805	678	669
C/MHz	685.62	798	648	767	696	595	588

Table 7 Direction cosines of the internal rotor axis with the inertial axes of the cluster, determined from the geometrical structure determination, *cf.* section 2.1

	Phenol $(CH_3OH)_1$		Phenol $(CD_3OH)_1$	
	S_0	S_1	S_0	S_1
B_a/MHz	3290.8	3310.5	3145.0	3170.3
B_b/MHz	792.19	775.89	746.6	730.49
B_c/MHz	685.62	664.25	654.6	630.74
D_a/MHz	32.83	78.90	3.82	12.49
D_b/MHz	14.3	38.2	0[a]	0[a]
D_c/MHz	40.31	52.13	6.95	36.83
λ_a	±0.028	±0.151	±0.049	±0.173
λ_b	±0.192	±0.087	±0.184	±0.099
λ_c	±0.981	±0.984	±0.982	±0.980
r	1	1	1	1
Δ_{AE}/MHz		3557.621		438.52

[a] Kept fixed, *cf.* section 2.

As pointed out before, the acidity of phenol increases strongly upon electronic excitation, thus the interaction of the methanolic oxygen lone pair with the phenolic proton is increased upon electronic excitation. Due to the increased hydrogen bond strength in the S_1-state, less electron density can be provided for the hyperconjugative effect. The smaller amount of hyperconjugation in the electronically excited state, thus leads to the observed reduction of the methyl torsional barrier in the S_1-state. This explanation for the decrease in barrier height upon electronic excitation is further supported by the work of Pophristic *et al.*[31] in which they determine the role of lone pairs in internal rotation barriers. They calculated the torsional barriers of dimethyl ether and protonated dimethyl ether and found a decrease of the barrier height from 2000 cm^{-1} to 400 cm^{-1} in a fully relaxed (with respect to all coordinates without the internal rotation) *ab initio* calculation.

Therefore we propose that the decrease of the torsional barrier in the methanol moiety upon electronic excitation in the phenol moiety is a direct consequence of the increased S_1-state acidity of phenol. This hypothesis will be tested using substituted phenols, which are strong photoacids (*e.g.* 4-cyanophenol) and should show a more pronounced effect on the torsional barrier upon electronic excitation. The pK_a value of 4-cyanophenol was determined to be 7.74 in the S_0-state and 3.33 in the S_1-state,[32] thus it is a stronger acid compared to phenol (9.82 and 6, respectively) in both electronic states and shows a larger increase of acidity upon electronic excitation. It should therefore be an ideal candidate for a check of the above hypothesis.

Acknowledgements

We would like to thank especially Professor Karl Kleinermanns for his steady interest in this work and for many helpful discussions. The authors are indebted to Dr Michel Mons for making the semi-empirical structure of phenol–methanol available to us. The financial support of the Deutsche Forschungsgemeinschaft (SCHM 1043/9-2 and 9-4) is gratefully acknowledged.

References

1 H. Abe, N. Mikami and M. Ito, *J. Phys. Chem.*, 1982, **86**, 1768.
2 H. Abe, N. Mikami, M. Ito and Y. Udagawa, *J. Phys. Chem.*, 1982, **86**, 2567.
3 T. G. Wright, E. Cordes, O. Dopfer and K. Müller-Dethlefs, *J. Chem. Soc., Faraday Trans.*, 1993, **89**, 1601.
4 M. Gerhards, K. Beckmann and K. Kleinermanns, *Z. Phys. D*, 1994, **29**, 223.
5 M. Schmitt, H. Müller, U. Henrichs, M. Gerhards, W. Perl, C. Deusen and K. Kleinermanns, *J. Chem. Phys.*, 1995, **103**, 584.
6 A. Courty, M. Mons, B. Dimicoli, F. Piuzzi, V. Brenner and P. Millié, *J. Phys. Chem. A*, 1998, **102**, 4890.
7 C. Plützer, C. Jacoby and M. Schmitt, *J. Phys. Chem. A*, 2002, **106**, 3998.
8 U. Gudladt, *Mikrowellenspektroskopische Untersuchungen des Komplexes phenol–methanol*, PhD thesis, Christian Albrechts Universität, Kiel, 1996.
9 M. Schmitt, J. Küpper, D. Spangenberg and A. Westphal, *Chem. Phys.*, 2000, **254**, 349.
10 J. Küpper, A. Westphal and M. Schmitt, *Chem. Phys.*, 2001, **263**, 41.
11 C. Ratzer, J. Küpper, D. Spangenberg and M. Schmitt, *Chem. Phys.*, 2002, **283**, 153.
12 J. K. G. Watson, *J. Chem. Phys.*, 1967, **46**, 1935.
13 J. K. G. Watson, *J. Chem. Phys.*, 1968, **48**, 4517.
14 W. Gordy and R. L. Cook, *Microwave Molecular Spectra*, 3rd edn., Wiley, New York, 1984.
15 D. R. Herschbach, *J. Chem. Phys.*, 1959, **31**, 91.
16 N. W. Larsen, *J. Mol. Struct.*, 1979, **51**, 175.
17 M. C. L. Gerry, R. M. Lees and G. Winnewisser, *J. Mol. Spectrosc.*, 1976, **61**, 231.
18 H. D. Rudolph, *Struct. Chem.*, 1991, **2**, 581.
19 J. K. G. Watson, *J. Mol. Spectrosc.*, 1973, **48**, 479.
20 J. G. Smith and J. K. G. Watson, *J. Mol. Spectrosc.*, 1978, **69**, 47.
21 J. K. G. Watson, A. Roytburg and W. Ulrich, *J. Mol. Spectrosc.*, 1999, **196**, 102.
22 J. K. G. Watson, *J. Mol. Spectrosc.*, 2001, **207**, 16.
23 M. J. Frisch, G. W. Trucks, H. B. Schlegel, G. E. Scuseria, M. A. Robb, J. R. Cheeseman, V. G. Zakrzewski, J. A. Montgomery, Jr., R. E. Stratmann, J. C. Burant, S. Dapprich, J. M. Millam, A. D. Daniels, K. N. Kudin, M. C. Strain, O. Farkas, J. Tomasi, V. Barone, M. Cossi, R. Cammi, B. Mennucci, C. Pomelli, C. Adamo, S. Clifford, J. Ochterski, G. A. Petersson, P. Y. Ayala, Q. Cui, K. Morokuma, P. Salvador, J. J. Dannenberg, D. K. Malick, A. D. Rabuck, K. Raghavachari, J. B. Foresman, J. Cioslowski, J. V. Ortiz, A. G. Baboul, B. B. Stefanov, G. Liu, A. Liashenko, P. Piskorz, I. Komaromi, R. Gomperts, R. L. Martin, D. J. Fox, T. Keith, M. A. Al-Laham, C. Y. Peng, A. Nanayakkara, M. Challacombe, P. M. W. Gill, B. Johnson, W. Chen, M. W. Wong, J. Andres, C. Gonzalez, M. Head-Gordon, E. S. Replogle and J. A. Pople, *Gaussian 98, Revision A.11*, *Gaussian, Inc.*, Pittsburgh, PA, 2001.
24 S. Simon, M. Duran and J. J. Dannenberg, *J. Chem. Phys.*, 1996, **105**, 11 024.
25 E. B. Wilson, Jr., C. C. Lin and D. R. Lide, Jr., *J. Chem. Phys.*, 1955, **23**, 136.
26 K. Levenberg, *Q. Appl. Math.*, 1944, **2**, 164.
27 D. D. Marquardt, *J. Soc. Ind. Appl. Math.*, 1963, **11**, 431.
28 C. Jacoby and M. Schmitt, 2003, in preparation.
29 J. Lorentzon, P.-A. Malmqvist, M. Fülscher and B. Roos, *Theor. Chim. Acta*, 1995, **91**, 91.
30 V. Pophristic and L. Goodman, *J. Phys. Chem. A*, 2002, **106**, 1642.
31 V. Pophristic, L. Goodman and N. Guchhait, *J. Phys. Chem. A*, 1997, **101**, 4290.
32 S. Schulman, W. Vincent and W. Underberg, *J. Phys. Chem.*, 1981, **85**, 4068.
33 J. K. G. Watson, *J. Mol. Spectrosc.*, 1977, **66**, 500.